Drug Design, Development and Therapy Dovepress

Open Access Full Text Article ORIGINAL RESEARCH

Discovery of a Novel and Potent Dual-Targeting Inhibitor of ATM and HDAC2 Through Structure-Based Virtual Screening for the Treatment of Testicular Cancer

Yashi Ruan[1,*], Lixia Guan[2,*], Yuting Wang[2], Yifei Geng[2], Xiaoran Wang[2], Miao-Miao Niu[2], Li Yang[1], Cen Xu[1], Zhen Xu[1]

[1]Department of Urology, Reproductive Medicine and Oncology, The Affiliated Taizhou People's Hospital of Nanjing Medical University, Taizhou, 225300, People's Republic of China; [2]Department of Pharmaceutical Analysis, China Pharmaceutical University, Nanjing, 211198, People's Republic of China

*These authors contributed equally to this work

Correspondence: Li Yang; Cen Xu, Department of Urology, Reproductive Medicine and Oncology, The Affiliated Taizhou People's Hospital of Nanjing Medical University, Taizhou, 225300, People's Republic of China, Email proyangli@163.com; cenxu263128@163.com

Purpose: Dual inhibition of ataxia telangiectasia mutated (ATM) and histone deacetylase 2 (HDAC2) may be a potential strategy to improve antitumor efficacy in testicular cancer.

Methods: A combined virtual screening protocol including pharmacophore modeling and molecular docking was used for screening potent dual-target ATM/HDAC2 inhibitors. In order to obtain the optimal lead compound, the dual ATM/HDAC2 inhibitory activity of the screened compounds was further evaluated using enzyme inhibition methods. The binding stability of the optimal compound to the dual targets was verified by molecular dynamics (MD) simulation. MTT assay and in vivo antitumor experiment were performed to validate antitumor efficacy of the optimal compound in testicular cancer.

Results: Here, we successfully discovered six potent dual-target ATM/HDAC2 inhibitors (AMHs 1–6), which exhibited good inhibitory activity against both ATM and HDAC2. Among them, AMH-4 showed strong inhibitory activity against both ATM (IC_{50} = 1.12 ± 0.03 nM) and HDAC2 (IC_{50} = 3.04 ± 0.08 nM). MD simulation indicated that AMH-4 binds to ATM and HDAC2 with satisfactory stability. Importantly, AMH-4 had significant antiproliferative activity on human testicular tumor cells, especially NTERA-2 cL.D1 cells, and no inhibitory effect on normal human testicular cells. In vivo experiments exhibited that AMH-4 was more effective than lartesertib and vorinostat in inhibiting the growth of NTERA-2 cL.D1 xenograft tumors with low toxicity.

Conclusion: Overall, these results suggest that AMH-4 is an effective and low toxicity candidate for the treatment of testicular germ cell tumors.

Keywords: ataxia telangiectasia mutated, histone deacetylase 2, dual-targeting inhibitors, testicular germ cell tumors, structure-based virtual screening

Introduction

Testicular germ cell tumors (TGCT) are the most common type of testicular malignancy, emerging most frequently in males between the ages of 15 and 40.[1,2] During the past 20 years, the incidence of testicular cancer has continued to rise in many countries and is expected to increase further in the future.[3,4] Currently, surgery and standard-dose chemotherapy are the main methods of treating TGCT.[5] Approximately 80–90% of metastatic TGCT have a high cure rate after standard dose cisplatin chemotherapy.[5] However, testicular cancer survivors treated with cisplatin face many toxic side effects, including ototoxicity, neuropathy, cardiovascular toxicity, infertility, and secondary malignancies.[6] In addition, young patients may face a range of long-term psychosocial issues after treatment, including mental health, gender

Received: 20 May 2024
Accepted: 28 October 2024
Published: 20 November 2024

relations and work issues, which can significantly affect their overall quality of life.[7] For TGCT-resistant patients who have failed multiple chemotherapy regimens, the clinical cure rate is extremely low.[6] Therefore, the development of novel drugs for testicular cancer is indeed urgent. At present, dual-target therapy is a promising treatment strategy with fewer side effects, lower toxicity, and the potential to overcome drug resistance in cancer treatment.[8–10]

ATM plays a central role in protecting the genome from DNA damage through intact DNA repair pathways.[11–13] There are growing evidences suggest that ATM can coordinate homologous recombination (HR) and non-homologous end joining (NHEJ) pathways to repair DNA double-strand breaks (DSBs) and maintain genomic integrity.[11,14,15] In response to DSBs, ATM kinase undergoes self-phosphorylation and subsequently phosphorylates several downstream substrates, including p53, p21, Nbs1, and KAP1, ultimately mediating DNA repair and cell cycle regulation.[12,16,17] Studies have shown that abnormal ATM, characterized by serine 1981 phosphorylation, can be observed in testicular germ cell tumors.[18] Therefore, the inhibition of ATM represents a potential therapeutic strategy in testicular cancer treatment. Despite recent advances in ATM inhibitors, such as lartesertib,[19] AZD1390,[20] and KU60019[21] (Figure 1), toxicity and drug resistance cannot be ignored. There are currently no ATM inhibitors specifically for testicular cancer. Thus, it is urgent to develop novel ATM inhibitors with good drug properties and few side effects.

HDAC2, a member of the HDAC family, has been shown to be closely associated with tumor proliferation.[22–24] Overexpression of HDAC2 can increase deacetylation and cause an imbalance in the expression of certain cell cycle regulators, leading to cancer initiation and progression.[25–27] HDAC2 regulates the expression of a variety of genes and promotes cancer progression by silencing the expression of pro-apoptotic proteins (such as NOXA and APAF1) and inactivating the tumor suppressor p53.[28,29] In several types of cancer, high levels of HDAC2 expression are closely associated with tumor development, and may contribute to the development of resistance to cancer therapies.[30] Thus, HDAC2 is considered to be a potential target for cancer therapy because of its role in tumorigenesis.[31] Currently, some HDAC inhibitors are already used in clinical cancer treatment, including vorinostat, romidepsin, and belinostat (Figure 1).[32–34] However, most of these drugs are pan HDAC inhibitors and have similar dose-limiting toxicity.[35,36] So the development of specific HDAC2 inhibitors is particularly important.

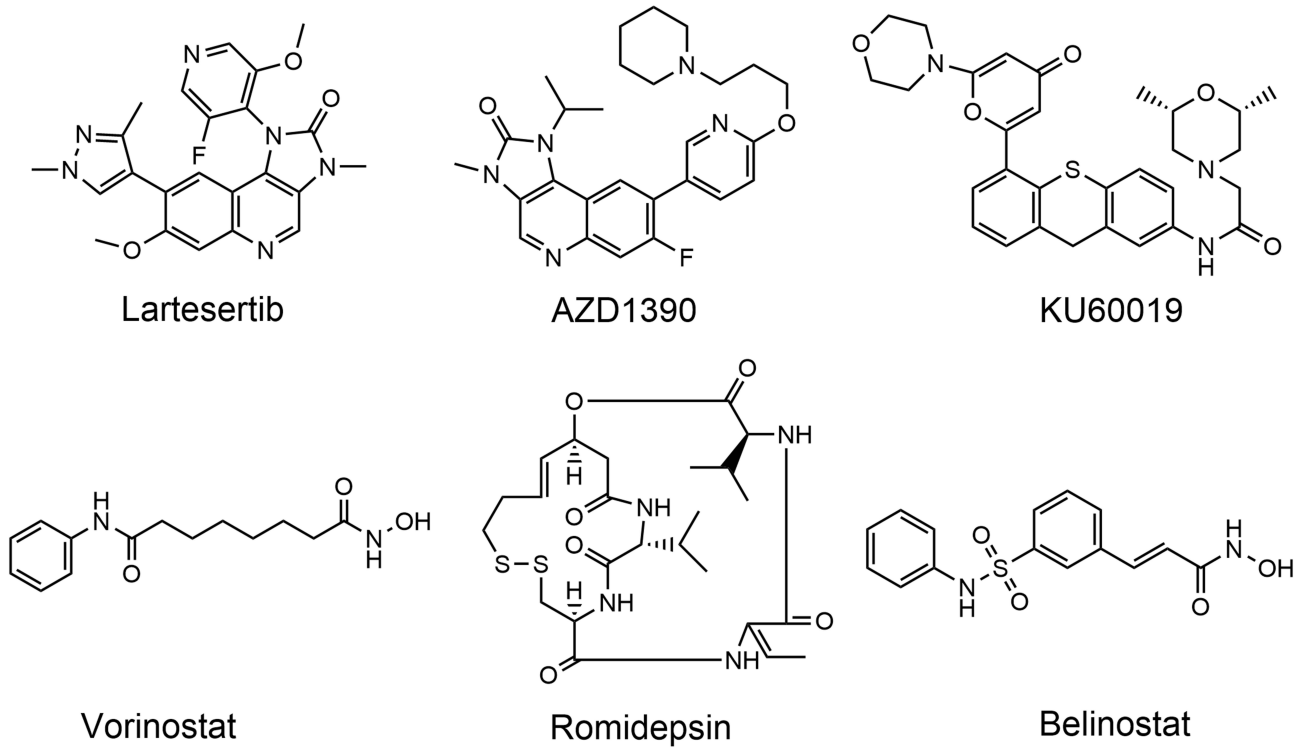

Figure 1 Reported ATM and HDAC inhibitors.

A recent study has shown that the combination of the ATM inhibitor KU60019 and the HDAC inhibitor romidepsin produces more effective cytotoxic effects in lymphoma cell lines than either drug alone.[37] Moreover, clinical studies have shown that HDAC inhibitors can reduce ATM-mediated activation of DNA damage signaling in a variety of tumor cells.[38] Thus, the combination of HDAC inhibitors and ATM inhibitors may synergistically cause insufficient DDR induction in tumor cells to enhance antitumor activity.[38] Although the combination of two drugs shows favourable therapeutic effects, the different drugs result in non-overlapping resistance mechanisms and different toxicities.[39,40] Compared to combination therapies, dual-target drugs with a single chemical entity may reduce the risk of drug-drug interactions, decrease toxicity and improve patient compliance.[39,40] Thus, dual-target ATM/HDAC2 inhibitors are potential therapeutic agents for the treatment of testicular cancer. To date, there are no reports of dual-target ATM/HDAC2 inhibitors.

Structure-based virtual screening is a computational approach to discovery lead compounds that is more cost-effective than traditional high-throughput screening.[41] The combined screening of the pharmacophore models and molecular docking can effectively identify potential drug candidates against specific targets.[42,43] In previous studies, we have successfully discovered some new and potent dual-target inhibitors through a comprehensive virtual screening scheme: PLK1/PLK4, NRP1/KRAS^{G12D}, tubulin/PARP-1.[9,41,44] Here, we identified novel dual-target ATM/HDAC2 inhibitors (AMHs 1–6) through a combined virtual screening protocol. Among them, AMH-4 had the highest inhibitory activity on both ATM and HDAC2. Meanwhile, AMH-4 showed significant in vitro antiproliferative and in vivo antitumor activity in testicular cancer with low toxicity. In conclusion, the dual-targeted ATM/HDAC2 inhibitor AMH-4 is a promising therapeutic candidate for the treatment of testicular cancer.

Materials and Methods

Cell Culture and Materials

The human testicular germ cell tumors (TGCT) cell lines (NTERA-2 cL.D1, Cates-1B, Tera-1) and human normal testicular cell line (Hs 1.Tes) were purchased from the American Type Culture Collection (ATCC, Manassas, VA, USA). The cells were cultured with Dulbecco's modified Eagle medium (DMEM, Gibco BRL, Grand Island, NY, USA) supplemented with 10% (v/v) fetal bovine serum, 100 units/mL of penicillin, and 100 μg/mL of streptomycin. The cell culture system was maintained at 37°C in a humidified atmosphere containing 5% CO_2. Hit compounds (AMHs 1–6) were purchased from WuXi AppTec (Shanghai, China), the vendor name and ID of AMHs 1–6 are listed in Table S1. Recombinant human ATM and HDAC2 proteins were purchased from Abcam (Cambridge, MA, USA).

Virtual Screening

The crystal structures of ATM (PDB ID: 7NI4) and HDAC2 (PDB ID: 4LXZ) proteins were obtained from the Protein Data Bank (PDB). The two crystal structures were imported into the Molecular Operating Environment (MOE, Chemical Computing Group Inc, Montreal, Quebec, Canada). The QuickPrep tool of MOE was used for structural preparation, including the deletion of distant solvent and the addition of hydrogen atoms. Then, the energy was minimized through Amber14: EHT force field. Based on combinatorial chemistry methods, we have established a database of 43,000 compounds. The Ligand interactions tool in MOE was used to construct pharmacophore models based on the ATM crystal structure, including hydrogen bond donor, hydrogen bond acceptor, aromatic center and hydrophobic centroid. The established pharmacophore model was then used for virtual screening to determine the screening results in terms of root mean square deviation (RMSD) values.

Next, the selected compounds were further subjected to molecular docking based on the above crystal structures of ATM and HDAC2. The ligand atoms were used to define active sites within the 5 Å region, and the docking was determined using the Triangle Matcher method and London dG scoring algorithm. Typically, lower docking scores reflect higher binding affinity.

In vitro ATM Inhibition Assay

The inhibition assay was conducted according to previously reported methods.[45] First, ATM enzyme was mixed with Hepes buffer (50 mm Hepes pH 7.4, 150 mm NaCl, 10 mm $MnCl_2$, 1 mm DTT, 5% v/v Glycerol, 0.05% v/v Tween 20). The mixture was incubated with DMSO-dissolved compounds for 0.5 h. After the addition of a substrate solution of p53 (5 μM) and ATP (50 nM) for 2 h, the reaction was terminated by the addition of detection reagent (33 mm Hepes pH 7.4, 20 mm EDTA, 0.1 M KF, 0.1 mg/mL BSA, 13 nM D2 Anti-GST antibody (Cisbio) and 0.5 nM Eu^{3+} Anti-p53phosphoS15 antibody). Finally, the values were obtained on the PHERAstar instrument (BMG Labtech, Cary, NC) with the standard Homogeneous Time-Resolved Fluorescence (HTRF) filter block method. IC_{50} values were determined using the data analysis software Genedatascreener®.

In vitro HDAC2 Inhibition Assay

The method was performed as described previously.[46] In brief, a mixture of 10 μL HDAC2 enzyme solutions and 50 μL mixed with various concentrations of inhibitor compounds was added to a 96-well plate and incubated for 5 min at 37 ° C. Next, the fluorescent substrate Boc-Lys (acetyl) -AMC (40 μL) was injected into each well and incubated for 0.5 h. The mixture was maintained for 20 min with 100 μL of developer containing trypsin and TSA. Finally, the fluorescence intensity at wavelengths of 390 and 460 nm was measured by a microplate reader (BioTek Cytation 5; Agilent Technologies, Inc., Santa Clara, CA, USA).

MD Simulation

The structures of ATM (PDB ID: 7NI4) and HDAC2 (PDB ID: 4LXZ) were downloaded from the PDB. MD simulation was performed using GROMACS (version 2021.5) with the AMBER99SB ILDN force field. AMH-4 was imported into the Acpype Server (www.bio2byte.be) to obtain topology parameter files under the GAFF force field. Firstly, the system was dissolved in a 1.0 nm cubic box using SPC/E water models. Then, the sodium ions (Na^+) and chloride ions (Cl^-) were added to the system to maintain a neutral charge state. Subsequently, a 5000 step steepest descent algorithm was used for energy minimization. A V-type thermostat was used for 100 ps NVT balance to maintain system temperature at 300 K, and a 100 ps NPT simulation was performed by Parrinello Rahman barometer for further to maintain system pressure at 1 bar. Finally, a 50 ns MD simulation was conducted on the system and trajectory data was recorded at intervals of 10 ps. These data were processed using GraphPad Prism 6.0 software.

MTT Experiment

The MTT assay was performed as previously described.[9] In this experiment, four types of cells were measured (NTERA-2 cL.D1, Cats-1B, Tera-1, and Hs1.Tes). The cells were seeded in 96-well plates at a density of 5×10^4 cells/well and cultured overnight, respectively. Then AMH-4 at the various concentrations was added to each well and incubated at 37 ° C for 72 hours. Subsequently, the culture medium was removed and MTT solution (5mg/mL) was added to each well and incubated for another 4 hours. Then the supernatant was discarded and insoluble crystals were dissolved in dimethyl sulfoxide (DMSO). Finally, a microplate reader was used to detect absorbance at 570 nm. The dose-response curve was drawn using GraphPad Prism 6.0 software (GraphPad Software Inc., San Diego, CA) to determine the value of the half maximal inhibitory concentration (IC_{50}).

In vivo Antitumor Assay

Male nu/nu mice (4–6 weeks old) were purchased from Changzhou Cavens Experimental Animal Limited Company (Changzhou, China). Mice were injected subcutaneously with NTERA-2 cL.D1 human testicular tumor cells suspended in PBS (200 μL, 1×10^7 cells). The tumors of 90–120mm^3 were generated in the bodies of the mice. The mice were randomly divided into four groups and daily intraperitoneal injection with vehicle, lartesertib, vorinostat and AMH-4, all at a concentration of 10 mg/kg. Tumor volume and body weight were measured every 3 days for 15 days. The tumor volume was measured directly using vernier calipers and calculated according to the formula: (c × c × d)/2 (c, minimum

diameter; d, maximum diameter). All animal experiments used in this experiment have been approved by the Animal Ethics Committee of China Pharmaceutical University (permit number: 2023–03-018).

Results and Discussion

Pharmacophore Construction

The pharmacophore models were constructed based on the crystal structure of ATM (PDB ID: 7NI4) to identify novel dual-target ATM/HDAC2 inhibitors. The Pharmacophore Query Editor of MOE was used to generate the most representative pharmacophore models. As shown in Figure 2A, the generated pharmacophore models were composed of two Acc features (F1 and F2: hydrogen-bond acceptors) and two Aro features (F3 and F4: aromatics center). All of these features represented interaction points for ligand binding to ATM: (i) the F1 and F2 features formed hydrogen-bond interactions with the key amino acid residues Lys2717 and Cys2770; (ii) the F3 and F4 features formed hydrophobic interactions with hydrophobic residues, including Pro2699, Leu2715, Leu2722, Tyr2755, Leu2767, Trp2769, Ile2888. Therefore, the constructed pharmacophore models can be considered as key chemical features to discover new ATM/HDAC2 inhibitors.

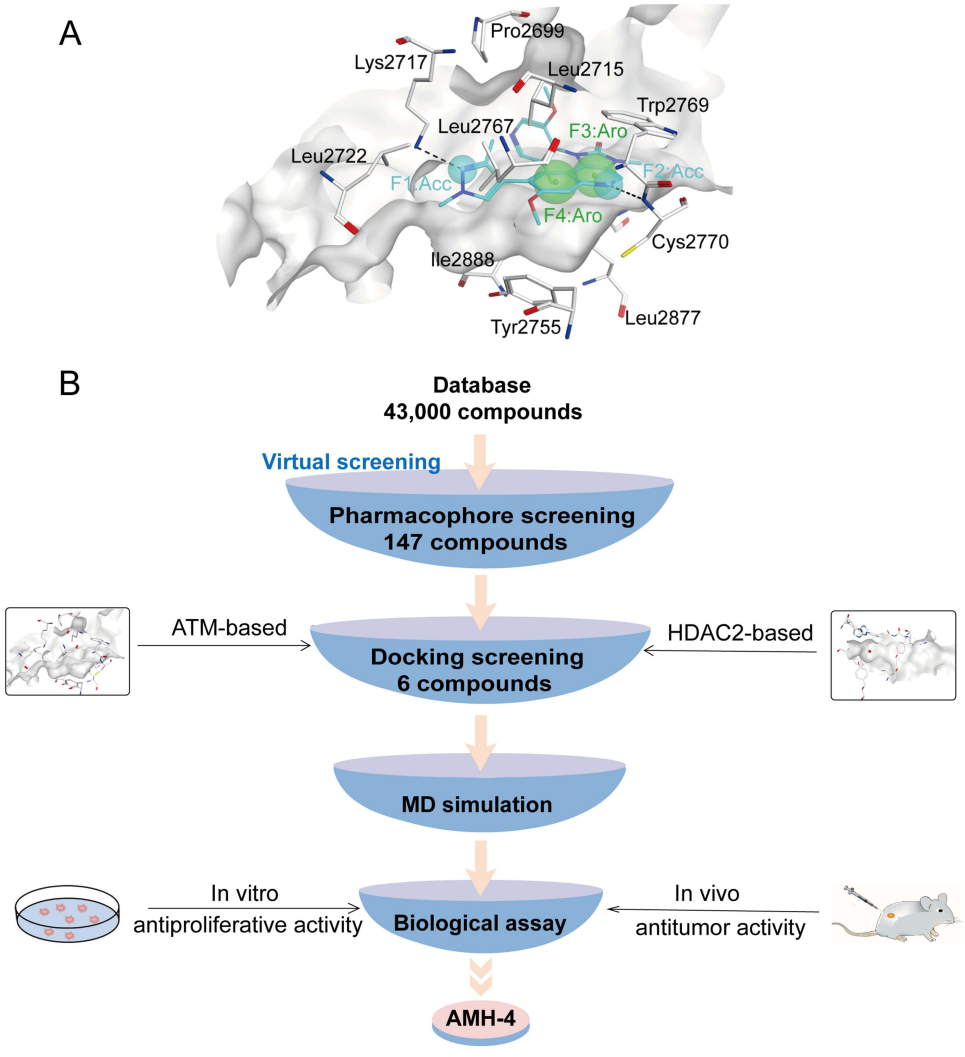

Figure 2 (**A**) The pharmacophore models based on the ATM structure. (**B**) The workflow of multi-step virtual screening of dual ATM/HDAC2 inhibitors.

Virtual Screening

In this study, a multi-step virtual screening process was used to identify potential dual-targeted ATM/HDAC2 inhibitors from an in-house database. The multi-step virtual screening workflow is shown in Figure 2B. Firstly, a two-dimensional (2D) database of 43,000 compounds was converted to a 3D structure. The constructed ATM pharmacophore models were used to screen the 3D database, resulting in the identification of 147 hit compounds with RMSD values less than 0.05 Å. Subsequently, these 147 screened hits were further docked to the active sites of ATM and HDAC2 to predict the binding affinities. The previously reported ATM inhibitor lartesertib and HDAC2 inhibitor vorinostat with a docking score of −12 kcal/mol were used as positive controls for the cutoff value. As shown in Figure 3, the docking values of six hits (AMHs 1–6) were less than −12 kcal/mol. Notably, AMH-4 had the lowest docking score of the six selected compounds, suggesting that it docked best with the active site of ATM/HDAC2. Based on the results of the above virtual screen, we further analyzed the interaction of six hit compounds with ATM/HDAC2. The chemical structures of the AMHs 1–6 are shown in Figure 4.

Interaction Analysis

The possible binding modes of the six selected hits (AMHs 1–6) at ATM and HDAC2 active sites were analyzed (Figures 5 and 6). Figure 5 shows the interaction analysis between AMHs 1–6 and ATM, respectively. We found that the pyridine and quinoxaline groups in the AMHs 1–6 formed hydrogen bonding interactions with key amino acid residues Lys2717 and Cys2770, while the benzene ring and alkyl group had hydrophobic interactions with Pro2699, Leu2715, Leu2722, Tyr2755, Leu2767, Trp2769, and Ile2888 in the hydrophobic cavity. Figure 6 shows the interaction analysis between AMHs 1–6 and HDAC2, respectively. The terminal N-hydroxyformamide group of AMHs 1–6 created an ionic bond with zinc ions in HDAC2 active sites. It is reported that the interaction between ligands and Zn^{2+} is crucial for enhancing the inhibitory activity of ligands against HDAC.[47] In particular, the N-hydroxyformamide group in each compound had three hydrogen bonds with His145, His146 and Tyr308, the urea group created hydrogen bonds with Lys205, while amino acid residues Tyr209 and Leu276 formed intermolecular hydrogen bonds. Meanwhile, the benzene ring and alkyl group had hydrophobic interactions with Phe155 and Phe210. Based on the above interaction analysis, we further investigated the biological activities of AMHs 1–6.

In vitro ATM and HDAC2 Inhibitory Activity

To evaluate the inhibitory effects of AMHs 1–6 on both ATM and HDAC2, the enzyme inhibition experiments were conducted. The ATM inhibitor lartesertib and HDAC2 inhibitor vorinostat served as positive controls. As shown in

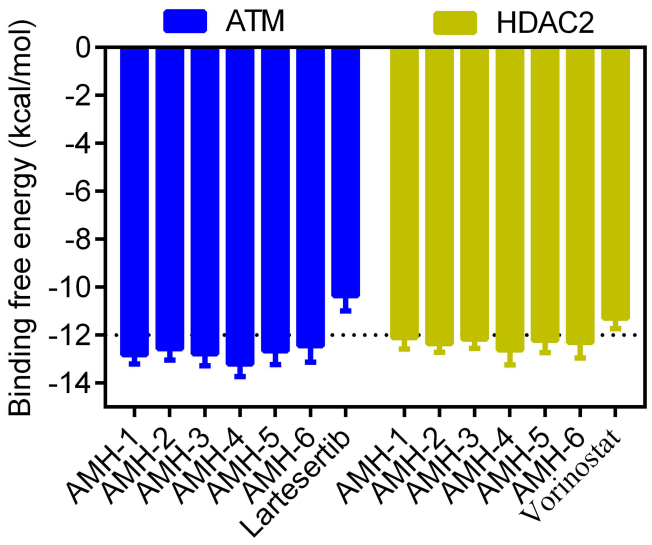

Figure 3 The binding free energy (kcal/mol) of six selected hit compounds (AMHs 1–6).

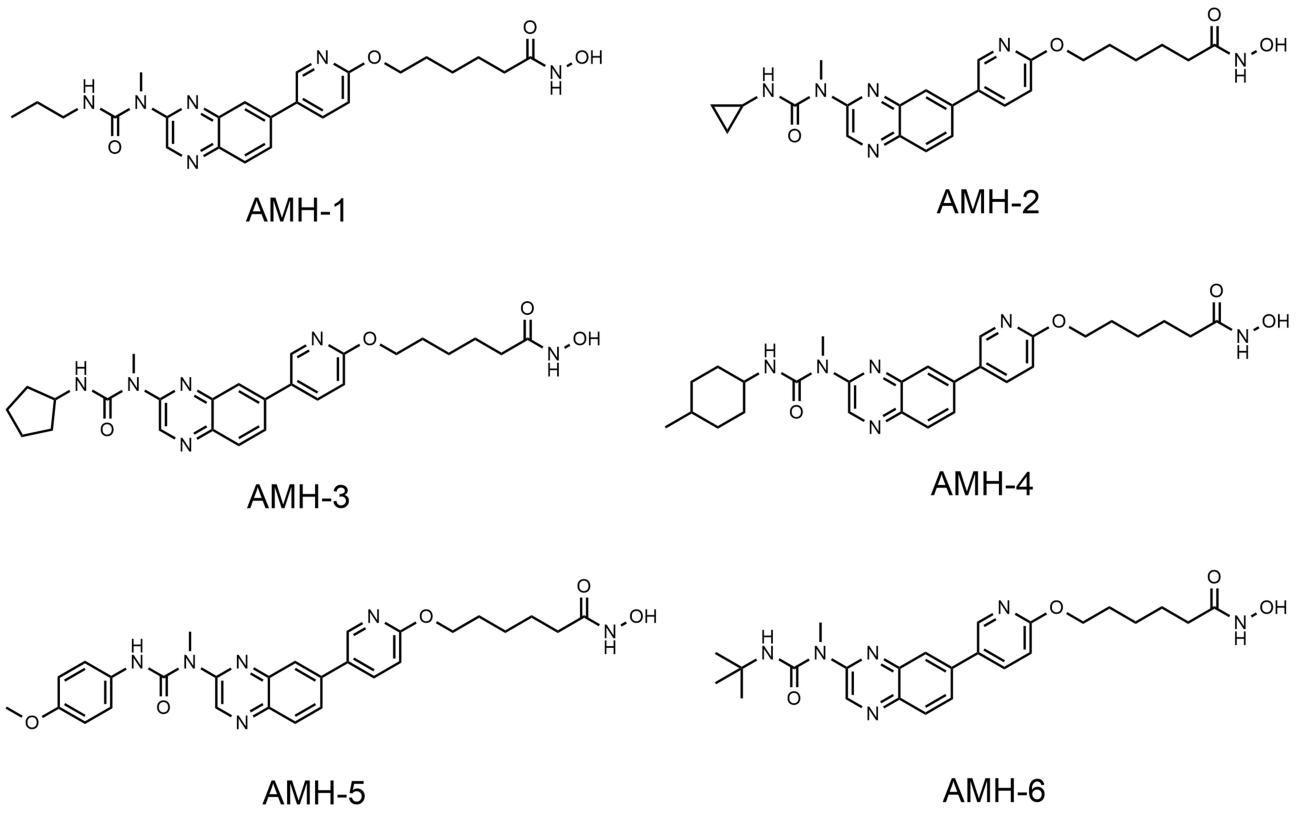

Figure 4 The chemical structures of six selected hit compounds (AMHs 1–6).

Table 1, we found that lartesertib had inhibitory activity on ATM (IC_{50} = 17.22 ± 3.39 nM), and no inhibitory effect on HDAC2. In contrast, vorinostat had inhibitory activity on HDAC2 (IC_{50} = 10.16 ± 2.75 nM), but did not affect ATM. AMHs 1–6 showed dual inhibition of both ATM and HDAC2, and the IC_{50} values of the six compounds were all lower than the positive controls. This indicated that AMH 1–6 had significant inhibitory activity against ATM and HDAC2. The IC_{50} values for inhibition of ATM by AMH 1–6 ranged from 1.12 nM to 9.68 nM, and those for inhibition of HDAC2 ranged from 3.04 nM to 9.27 nM. Notably, AMH-4 had the most potent inhibitory activity against both ATM (IC_{50} = 1.12 ± 0.03 nM) and HDAC2 (IC_{50} = 3.04 ± 0.08 nM), which was approximately 15-fold better than that of lartesertib (IC_{50} = 17.22 ± 3.39 nM), and about 3-fold better than that of vorinostat (IC_{50} = 10.16 ± 2.75 nM). The IC_{50} determination curves showed that AMH-4 significantly inhibited the activities of ATM and HDAC2 (Figure S1). In addition, AMH-4 exhibited the highest inhibitory activity, which was consistent with the docking score results. Therefore, AMH-4 is the most potent inhibitor for further in vitro cell viability evaluation.

MD Simulation

To assess the binding stability of AMH-4 at the ATM and HDAC2 active sites, we further analyzed the stability of the ATM-AMH-4 complex and HDAC2-AMH-4 complex systems within the 50 ns MD simulation using GROMACS (version 2021.5). The value of RMSD was calculated for the complex structure relative to the initial optimized structure. In Figure 7A and B, The RMSD of the ATM-AMH-4 complex initially increased and remained stable at around 0.35 nm after 30 ns; the RMSD of the HDAC2-AMH-4 complex remained steady at around 0.2 nm after 10 ns, indicating that AMH-4 can bind stably to ATM and HDAC2. In addition, to assess the flexibility of the amino acid residues in the complex, the root mean square fluctuation (RMSF) values were also calculated (Figure 7C and D). As shown in Figure 7C, the RMSF values of the key residues Pro2699, Leu2715, Lys2717, Leu2722, Tyr2755, Leu2767, Trp2769, Cys2770, and Ile2888 in the ATM active sites were all less than 0.2 nm throughout the simulation process, indicating that these key residues were stable in binding to AMH-4. In Figure 7D, the RMSF values of key residues His145, His146, Phe155, Lys205, Tyr209, Phe210,

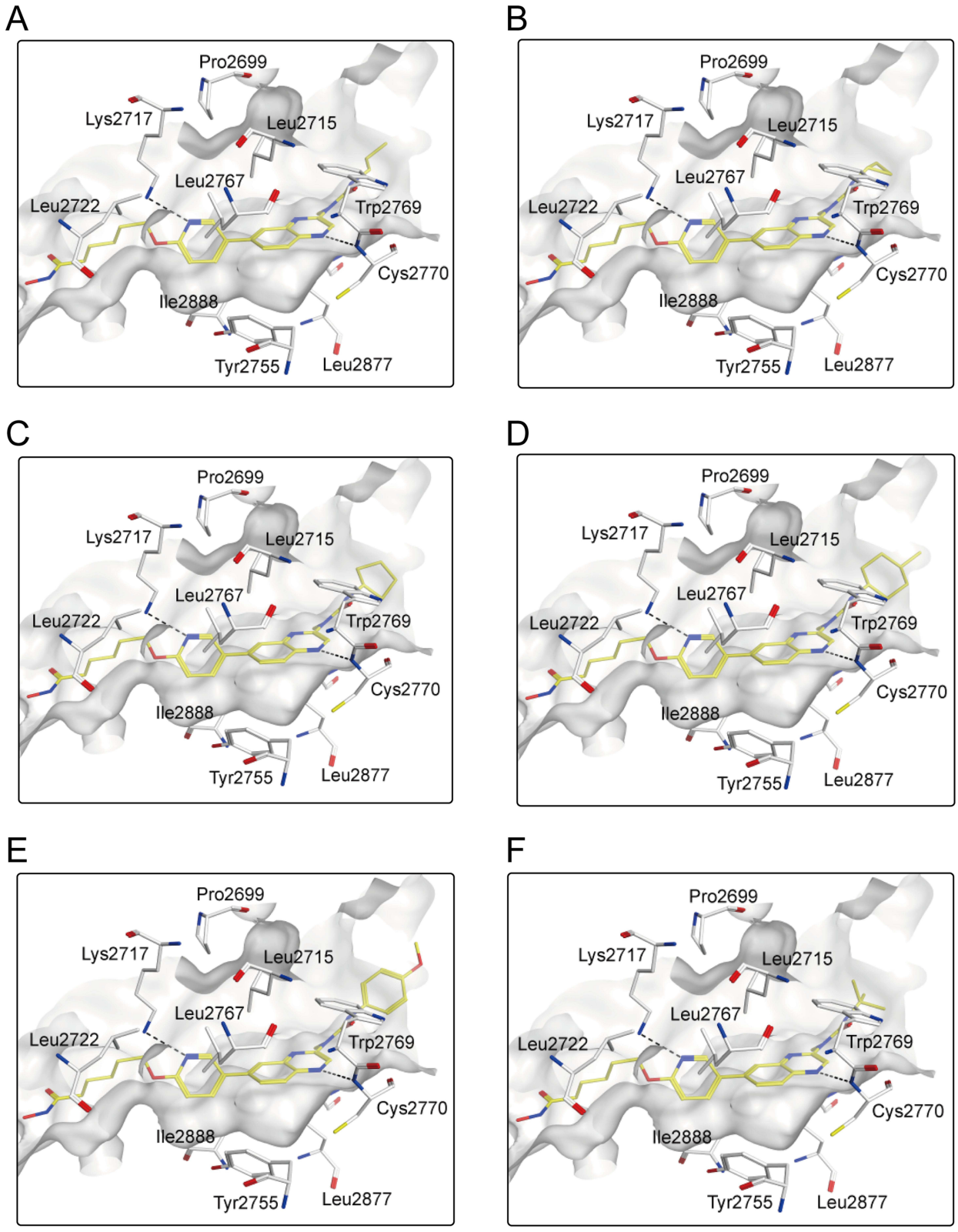

Figure 5 The binding modes of AMHs 1–6 (correspond to **A-F** respectively) in the active site of ATM. Residues in the active site are shown as white. AMHs 1–6 are coloured in yellow. The hydrogen bonds are represented in black dashed lines.

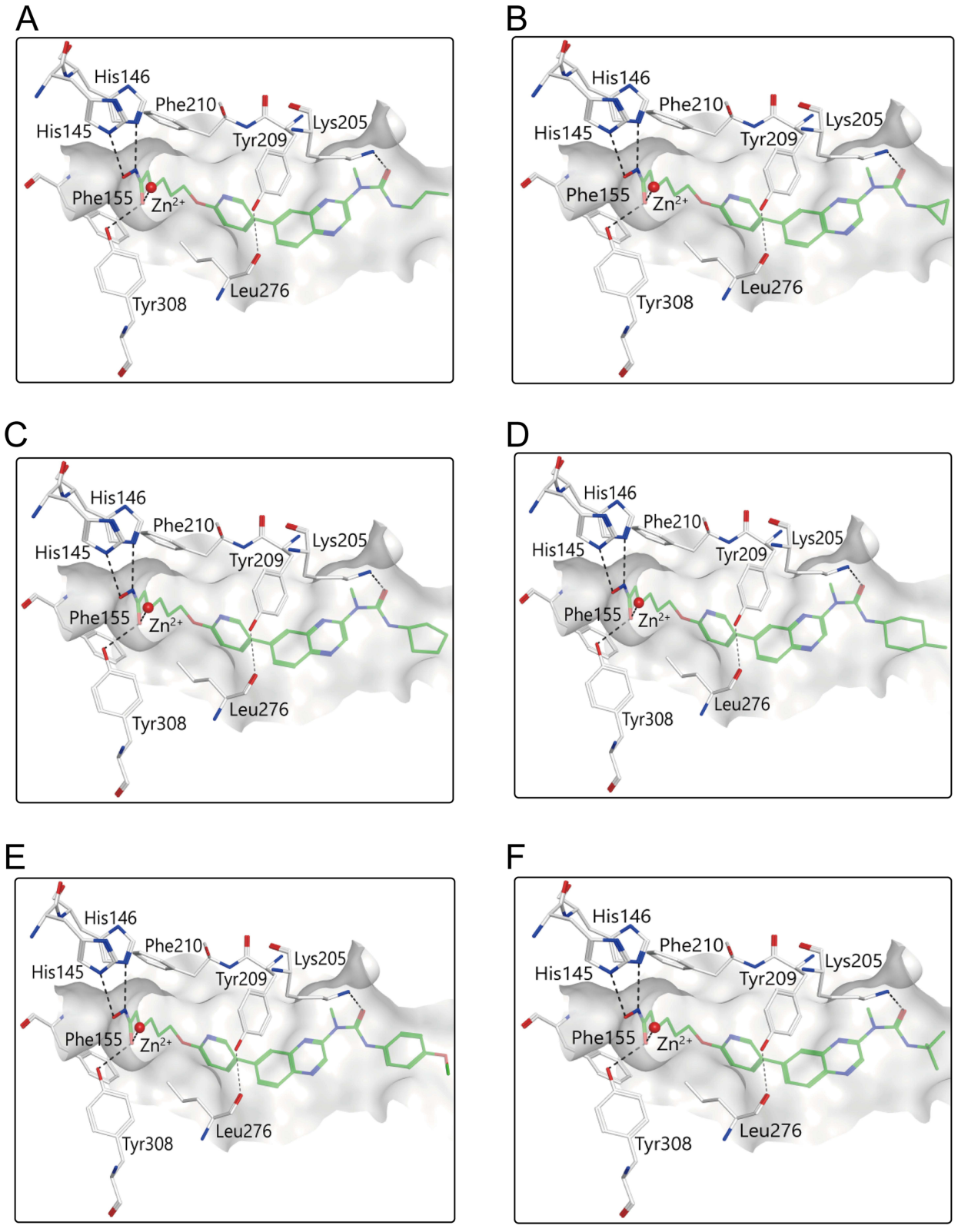

Figure 6 The binding modes of AMHs 1–6 (correspond to **A-F** respectively) in the active site of HDAC2. Residues in the active site are shown as white. AMHs 1–6 are coloured in green. The hydrogen bonds are represented in black dashed lines.

Table 1 The Inhibitory Effects of AMHs 1–6 and the Positive Controls on ATM and HDAC2

Compounds	ATM (IC_{50}, nM)	HDAC2 (IC_{50}, nM)
AMH-1	2.94 ± 0.26	9.27 ± 1.18
AMH-2	8.31 ± 1.05	5.11 ± 0.32
AMH-3	4.25 ± 0.71	8.52 ± 1.21
AMH-4	1.12 ± 0.03	3.04 ± 0.08
AMH-5	5.73 ± 0.92	7.61 ± 0.46
AMH-6	9.68 ± 2.84	6.09 ± 0.14
Lartesertib	17.22 ± 3.39	no inhibition
Vorinostat	no inhibition	10.16 ± 2.75

Leu276, and Tyr308 in the HDAC2 active site show small fluctuations in intensity less than 0.1 nm, reflecting a strong interaction with AMH-4. Finally, the stability of the system was evaluated by analysing the changes in the secondary structure of the protein during the 50 ns MD simulation process. As shown in Figure 7E and F, no significant changes were observed in the secondary structure of the protein, indicating the structural stability of ATM and HDAC2 in the complex. In conclusion, AMH-4 can stably bind to the active sites of ATM and HDAC2.

In vitro Antiproliferative Activity

To evaluate in vitro antiproliferative activity of AMH-4, we performed cytotoxicity studies on three human testicular tumor cell lines (NTERA-2 cL.D1, Cates-1B, Tera-1) and one human normal testicular cell line (Hs 1.Tes). The inhibitory effects of AMH-4 on above cells were detected using the MTT assay and IC_{50} values were calculated. As shown in Table 2, AMH-4 had significant antiproliferative activity on human testicular tumor cells, including NTERA-2 cL.D1, Cates-1 B and Tera-1. Notably, AMH-4 showed significant antiproliferative activity on NTERA-2 cL.D1 (IC_{50} = 0.12 μM) cells compared to Cates-1B (IC_{50} = 0.34 μM) and Tera-1 (IC_{50} = 0.25 μM) cells. Furthermore, AMH-4 had almost no inhibitory effect on the growth of normal human testicular cells Hs 1.Tes (IC_{50} > 10 μM), suggesting that AMH-4 has less toxic side effects. In addition, we evaluated the inhibition rate of AMH-4 on the four cell lines mentioned above. As shown in Figure S2, AMH-4 suppressed the proliferation of three types of testicular tumor cells in a dose-dependent manner, with the strongest inhibitory effect on NTERA-2 cL.D1 cells. Meanwhile, AMH-4 had no apparent inhibitory effect on the normal testicular cell line. In conclusion, AMH-4 potently inhibited the proliferation of testicular cancer cells, particularly NTERA-2 cL.D1 cells, with low toxicity to normal testicular cells. Therefore, we chose NTERA-2 cL.D1 as xenograft cells for in vivo antitumor study of AMH-4.

In vivo Antitumor Activity

Based on AMH-4 excellent antiproliferative activity in vitro, we evaluated the antitumor activity of AMH-4 in vivo in NTERA-2 cL.D1 xenograft models. Nude mice bearing tumor were randomly divided into four groups: vehicle, lartesertib, vorinostat and AMH-4, all at a concentration of 10 mg/kg. As shown in Figure 8A, all treatment groups inhibited tumour growth compared to the vehicle throughout the treatment period. Obviously, AMH-4 showed the most significant antitumor effect compared to the positive drugs vorinostat and lartesertib. In addition, the group of mice treated with AMH-4 showed a slight increase in body weight, while a slight decrease was observed in the groups treated with vorinostat (Figure 8B). Thus, these results suggest that AMH-4 has excellent antitumor activity against testicular cancer with low toxicity, suggesting its potential for the treatment of testicular cancer.

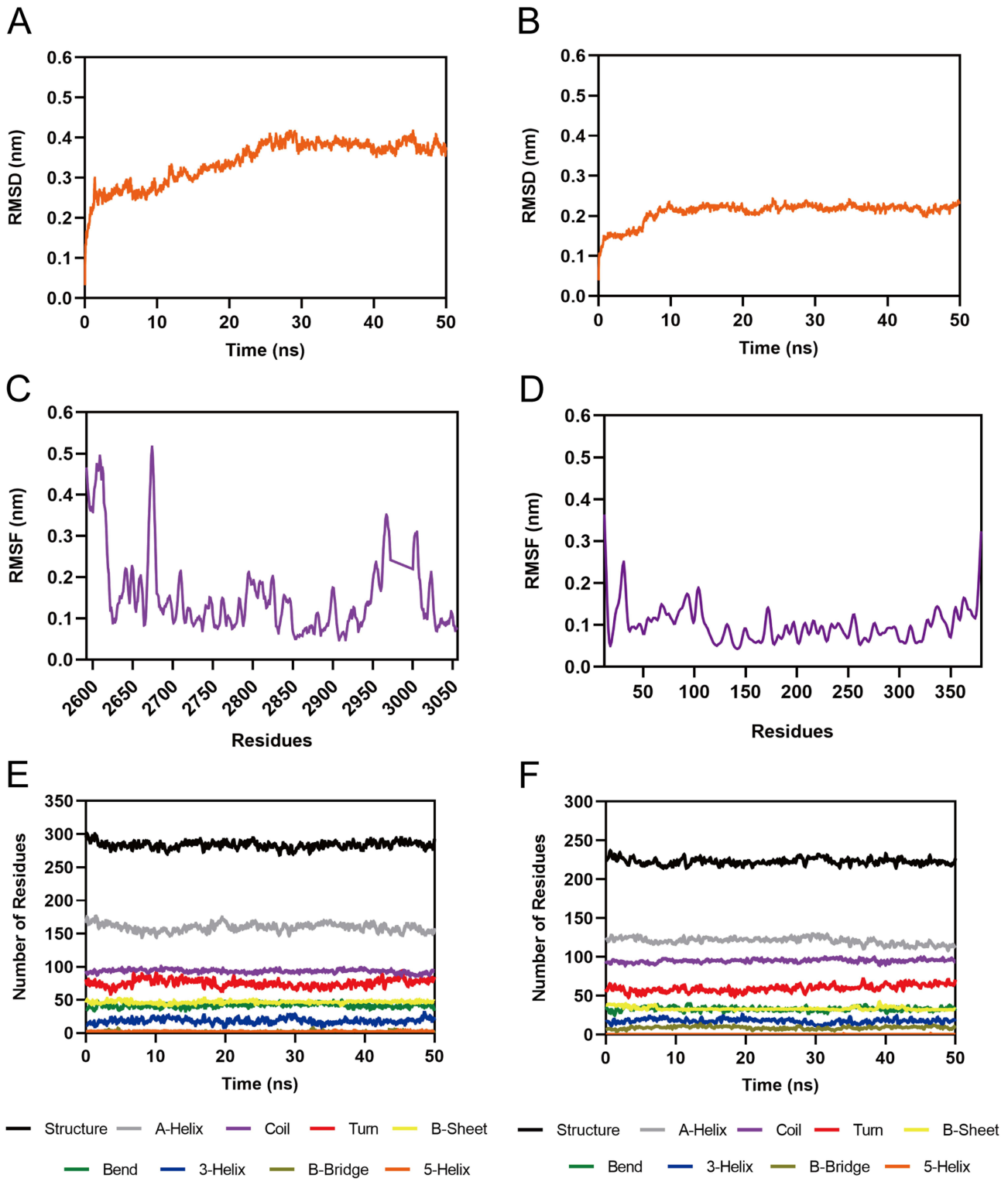

Figure 7 MD simulation of AMH-4 in complex with ATM and HDAC2. (**A**) The backbone RMSD of the complex of ATM and AMH-4. (**B**) The backbone RMSD of the complex of HDAC2 and AMH-4. (**C**) The RMSF of ATM Cα atoms in the complex of ATM and AMH-4. (**D**) The RMSF of HDAC2 Cα atoms in the complex of HDAC2 and AMH-4. (**E** and **F**) The secondary structures analysis of ATM and HDAC2, respectively.

Discussion

Despite significant advances in the treatment of testicular cancer, the range of physical and psychological health problems caused by current cancer treatments cannot be overlooked.[6,7] Therefore, the development of drugs with low toxicity and minimal side effects for the treatment of testicular cancer is essential. In testicular cancer, activation of ATM may

Table 2 The in vitro Cytotoxicity of AMH-4 on Human Testicular Tumor Cell Lines and Normal Human Testicular Cells

Name	IC_{50} (μM)[a]			
	NTERA-2 cL.D1	Cates-1B	Tera-1	Hs 1.Tes
AMH-4	0.12	0.34	0.25	>10

Note: [a]IC_{50} (μM) is the concentration of compound needed to reduce cell growth by 50% following 48 h cell treatment with AMH-4.

promote the survival and proliferation of tumor cells, while HDAC2 may influence tumor development by regulating gene expression.[18,30] In recent years, the development of dual-targeted inhibitors has been widely reported as a promising approach to improve drug efficacy or overcome resistance, and has become a popular area of research in cancer treatment.[48,49] Thus, inhibiting ATM and HDAC2 simultaneously may be an effective interventional strategy for testicular cancer treatment. However, due to the difference in the shape of the ATM and HDAC2 pockets, it is difficult to design inhibitors that target both ATM and HDAC2. In this study, we developed a series of ATM/HDAC2 dual-target inhibitor (AMHs 1–6) through a virtual screening approach based on pharmacophore screening and molecular docking. We have constructed pharmacophore models based on the structure of ATM (PDB ID: 7NI4) by identifying the key chemical features of active compounds, which are then used to screen large databases for compounds with similar features. Molecular docking was used to model the interactions between the compounds and the active binding site of ATM, from which potentially active compounds were screened. The combination of these two approaches can quickly, effectively and accurately screen out leads with greater potential. Subsequent biological evaluation showed that these compounds exhibited nanomolar inhibitory activity against ATM and HDAC2. In particular, AMH-4 with the lowest docking score identified by molecular docking showed excellent antitumor activity against testicular cancer both in vitro and in vivo. These results suggest that structure-based virtual screening is capable of identifying leads with biological activity and is a promising strategy in drug discovery and design. This provides a concrete foundation for future dual-target drug design.

Despite recent advances in ATM and HDAC inhibitors, achieving a balance between toxicity and efficacy remains a challenge. Lartesertib is a potent, orally bioavailable ATM inhibitor in Phase I clinical trials.[16] In clinical practice, the HDAC inhibitor vorinostat has shown dose-limited toxicity and tolerability.[50] In this study, AMH-4 showed greater efficacy and lower toxicity compared to the positive controls lartesertib and vorinostat in the treatment of testicular cancer. In a xenograft mouse model of testicular cancer, AMH-4 exhibited more potent antitumor effects and less toxicity than the positive controls. These results suggest that AMH-4 is a potential therapeutic candidate for testicular cancer. In the future, it is expected that AMH-4 will be modified to further increase its inhibitory potency in testicular cancer. In

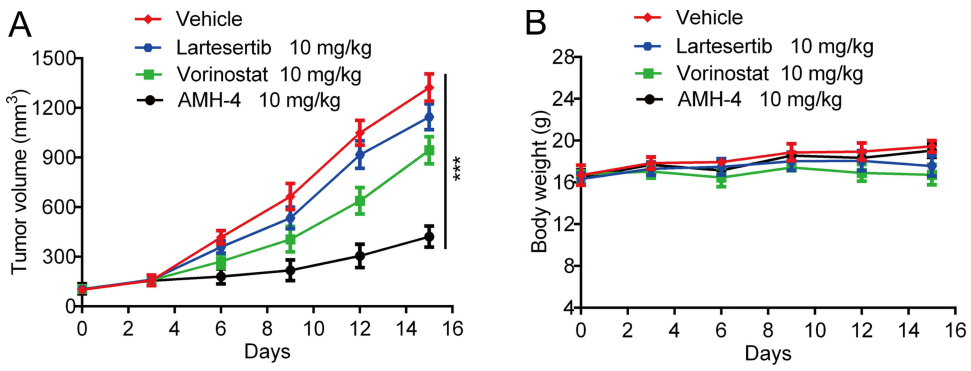

Figure 8 The antitumor activity of AMH-4 in NTERA-2 cL.D1 cell-derived xenografts. (**A**) Changes in tumor volume. (**B**) Body weight of mice. Data are presented as the mean ± SD, n = 6. ***$p < 0.001$ means a significant difference versus the vehicle group.

addition, dual-targeted drugs are often challenged by membrane permeability and safety issues, which is a direction for further optimization in the future.

Conclusions

Targeting both ATM and HDAC2 may offer new hope for the treatment of testicular cancer. In this study, a series of dual-targeting ATM/HDAC2 inhibitors (AMHs 1–6) were identified through a combined virtual screening protocol. The enzyme inhibition experiment showed that AMHs 1–6 had nanomolar inhibitory activities on both ATM and HDAC2. In particular, AMH-4 exhibited the most potent inhibitory effects. Meanwhile, MD simulation confirmed the stability of AMH-4 binding to ATM and HDAC2. Notably, AMH-4 had significant antiproliferative activity on human testicular tumor cells, and no inhibitory effect on normal human testicular cells. Furthermore, AMH-4 showed potent antitumor activity in a xenograft mouse model of testicular cancer. In conclusion, we have successfully discovered a novel and promising antitumor agent targeting ATM/HDAC2 for the treatment of testicular cancer.

Data Sharing Statement

The data used to support the findings of this study are available from the corresponding author upon request.

Ethical Statement

All procedures were conducted in accordance with the National Research Council's Guide for the Care and Use of Laboratory Animals. All experimental protocols were reviewed and approved by the Animal Ethics Committee of China Pharmaceutical University (permit number: 2023-03-018).

Funding

This research was supported by the Taizhou People's Hospital (Taizhou, Jiangsu, China; Grant No. ZL202220).

Disclosure

The authors report no conflicts of interest.

References

1. Weda S, Zweers D, Suelmann BBM, Meijer RP, Vervoort S. From surviving cancer to getting on with life: adult testicular germ cell tumor survivors' perspectives on transition from follow-up care to long-term survivorship. *Qualitative Health Research*. 2023;33(8–9):715–726. doi:10.1177/10497323231173808
2. Wu Z, Trabert B, Guillemette C, et al. Prediagnostic hormone levels and risk of testicular germ cell tumors: a nested case-control study in the janus serum bank. *Cancer Epidemiol Biomarkers Prev*. 2023;32(11):1564–1571. doi:10.1158/1055-9965.EPI-23-0772
3. Grasso C, Popovic M, Isaevska E, et al. Association study between polymorphisms in DNA methylation-related genes and testicular germ cell tumor risk. *Cancer Epidemiol Biomarkers Prev*. 2022;31(9):1769–1779. doi:10.1158/1055-9965.EPI-22-0123
4. Krasic J, Abramovic LS, Peric MH, et al. Testicular germ cell tumor tissue biomarker analysis: a comparison of human protein atlas and individual testicular germ cell tumor component immunohistochemistry. *Cells*. 2023;12(14):1841. doi:10.3390/cells12141841
5. Piulats JM, Vidal A, Garcia-Rodriguez FJ, et al. Orthoxenografts of testicular germ cell tumors demonstrate genomic changes associated with cisplatin resistance and identify PDMP as a resensitizing agent. *Clin Cancer Res*. 2018;24(15):3755–3766. doi:10.1158/1078-0432.CCR-17-1898
6. King J, Adra N, Einhorn LH. Testicular cancer: biology to bedside. *Cancer Res*. 2021;81(21):5369–5376. doi:10.1158/0008-5472.CAN-21-1452
7. Schepisi G, De Padova S, De Lisi D, et al. Psychosocial issues in long-term survivors of testicular cancer. *Front Endocrinol*. 2019;10:10. doi:10.3389/fendo.2019.00010
8. Zhang W, Pei J, Lai L. Computational multitarget drug design. *J Chem Inf Model*. 2017;57(3):403–412. doi:10.1021/acs.jcim.6b00491
9. Zheng L, Ren R, Sun X, et al. Discovery of a dual tubulin and poly(ADP-ribose) polymerase-1 inhibitor by structure-based pharmacophore modeling, virtual screening, molecular docking, and biological evaluation. *J Med Chem*. 2021;64(21):15702–15715. doi:10.1021/acs.jmedchem.1c00932
10. Ye J, Wu J, Liu B. Therapeutic strategies of dual-target small molecules to overcome drug resistance in cancer therapy. *Biochimica Et Biophysica Acta (BBA) - Reviews on Cancer*. 2023;1878(3):188866. doi:10.1016/j.bbcan.2023.188866
11. Dong C, Wang Y, Tu Z, et al. Recent advances in ATM inhibitors as potential therapeutic agents. *Future Med Chem*. 2022;14(23):1811–1830. doi:10.4155/fmc-2022-0252
12. Jang ER, Choi JD, Park MA, et al. ATM modulates transcription in response to histone deacetylase inhibition as part of its DNA damage response. *Exp. Mol. Med.* 2010;42(3):195–204. doi:10.3858/emm.2010.42.3.020
13. Dimitrov T, Moschopoulou AA, Seidel L, et al. Design and optimization of novel benzimidazole- and imidazo[4,5-b]pyridine-based atm kinase inhibitors with subnanomolar activities. *J Med Chem*. 2023;66(11):7304–7330. doi:10.1021/acs.jmedchem.2c02104

14. Kumar R, Cheok CF. RIF1: a novel regulatory factor for DNA replication and DNA damage response signaling. *DNA Repair*. 2014;15:54–59. doi:10.1016/j.dnarep.2013.12.004
15. Choi S, Srivas R, Fu KY, et al. Quantitative proteomics reveal ATM kinase-dependent exchange in DNA damage response complexes. *J Proteome Res*. 2012;11(10):4983–4991. doi:10.1021/pr3005524
16. Deng D, Yang Y, Zou Y, et al. Discovery and evaluation of 3-quinoxalin urea derivatives as potent, selective, and orally available ATM inhibitors combined with chemotherapy for the treatment of cancer via goal-oriented molecule generation and virtual screening. *J Med Chem*. 2023;66 (14):9495–9518. doi:10.1021/acs.jmedchem.3c00082
17. Wan R, Mo Y, Feng L, et al. DNA damage caused by metal nanoparticles: involvement of oxidative stress and activation of ATM. *Chem. Res. Toxicol.* 2012;25(7):1402–1411. doi:10.1021/tx200513t
18. Bartkova J, Bakkenist CJ, Rajpert-De Meyts E, et al. ATM activation in normal human tissues and testicular cancer. *Cell Cycle*. 2005;4(6):838–845. doi:10.4161/cc.4.6.1742
19. Fuchss T, Graedler U, Schiemann K, et al. Highly potent and selective ATM kinase inhibitor M4076: a clinical candidate drug with strong anti-tumor activity in combination therapies. *Cancer Res*. 2019;79(13):3500. doi:10.1158/1538-7445.AM2019-3500
20. Durant ST, Zheng L, Wang YC, et al. The brain-penetrant clinical ATM inhibitor AZD1390 radiosensitizes and improves survival of preclinical brain tumor models. *Sci Adv*. 2018;4(6). doi:10.1126/sciadv.aat1719.
21. Golding SE, Rosenberg E, Valerie N, et al. Improved ATM kinase inhibitor KU-60019 radiosensitizes glioma cells, compromises insulin, AKT and ERK prosurvival signaling, and inhibits migration and invasion. *Mol Cancer Ther*. 2009;8(10):2894–2902. doi:10.1158/1535-7163.MCT-09-0519
22. Al-Sanea MM, Gotina L, Mohamed MFA, et al. Design, synthesis and biological evaluation of new HDAC1 and HDAC2 inhibitors endowed with ligustrazine as a novel cap moiety. *Drug Des Devel Ther*. 2020;14:497–508. doi:10.2147/DDDT.S237957
23. Kalal BS, Pai VR, Behera SK, Somashekarappa HM. HDAC2 inhibitor valproic acid increases radiation sensitivity of drug-resistant melanoma cells. *Med Sci*. 2019;7(3):51. doi:10.3390/medsci7030051
24. Moreno-Yruela C, Fass DM, Cheng C, et al. Kinetic tuning of HDAC inhibitors affords potent inducers of progranulin expression. *ACS Chem. Neurosci.* 2019;10(8):3769–3777. doi:10.1021/acschemneuro.9b00281
25. Karaj E, Sindi SH, Kuganesan N, et al. First-in-Class Dual Mechanism Ferroptosis-HDAC Inhibitor Hybrids. *J Med Chem*. 2022;65 (21):14764–14791. doi:10.1021/acs.jmedchem.2c01276
26. Pham-The H, Casanola-Martin G, Dieguez-Santana K, et al. Quantitative structure-activity relationship analysis and virtual screening studies for identifying HDAC2 inhibitors from known HDAC bioactive chemical libraries. *Sar and Qsar in Environ Res*. 2017;28(3):199–220. doi:10.1080/1062936X.2017.1294198
27. Fang K, Dong G, Li Y, et al. Discovery of Novel Indoleamine 2,3-Dioxygenase 1 (IDO1) and Histone Deacetylase (HDAC) Dual Inhibitors. *ACS Med. Chem. Lett.* 2018;9(4):312–317. doi:10.1021/acsmedchemlett.7b00487
28. Han R, Ling C, Wang Y, Lu L. Enhancing HCC Treatment: innovatively combining HDAC2 inhibitor with PD-1/PD-L1 inhibition. *Can Cell Inter.* 2023;23(1). doi:10.1186/s12935-023-03051-0
29. Shetty MG, Pai P, Deaver RE, Satyamoorthy K, Babitha KS. Histone deacetylase 2 selective inhibitors: a versatile therapeutic strategy as next generation drug target in cancer therapy. *Pharmacol Res*. 2021;170.
30. Jo H, Shim K, Kim HU, Jung HS, Jeoung D. HDAC2 as a target for developing anti-cancer drugs. *Comput. Struct. Biotechnol. J.* 2023;21:2048–2057. doi:10.1016/j.csbj.2023.03.016
31. Yadav V, Banerjee S, Baidya SK, Adhikari N, Jha T. Applying comparative molecular modelling techniques on diverse hydroxamate-based HDAC2 inhibitors: an attempt to identify promising structural features for potent HDAC2 inhibition. *Sar and Qsar in Environ Res*. 2022;33(1):1–22. doi:10.1080/1062936X.2021.2013317
32. Richon VM, Garcia-Vargas J, Hardwick JS. Development of vorinostat: current applications and future perspectives for cancer therapy. *Cancer Lett*. 2009;280(2):201–210. doi:10.1016/j.canlet.2009.01.002
33. Bertino EM, Otterson GA. Romidepsin: a novel histone deacetylase inhibitor for cancer. *Expert Opin Invest Drugs*. 2011;20(8):1151–1158. doi:10.1517/13543784.2011.594437
34. Poole RM. Belinostat: first global approval. *Drugs*. 2014;74(13):1543–1554. doi:10.1007/s40265-014-0275-8
35. Shah RR. Safety and tolerability of histone deacetylase (HDAC) inhibitors in oncology. *Drug Safety*. 2019;42(2):235–245. doi:10.1007/s40264-018-0773-9
36. Suresh P, Devaraj V, Srinivas NR, Mullangi R. Review of bioanalytical assays for the quantitation of various HDAC inhibitors such as vorinostat, belinostat, panobinostat, romidepsin and chidamine. *Biomed. Chromatogr.* 2017;31(1):e3807. doi:10.1002/bmc.3807
37. Scotto L, Serrano XJ, Zullo K, et al. ATM inhibition overcomes resistance to histone deacetylase inhibitor due to p21 induction and cell cycle arrest. *Oncotarget*. 2020;11(37):3432–3442. doi:10.18632/oncotarget.27723
38. Suraweera A, O'Byrne KJ, Richard DJ. Combination Therapy With Histone Deacetylase Inhibitors (HDACi) for the Treatment of Cancer: achieving the Full Therapeutic Potential of HDACi. *Front Oncol*. 2018;8:8. doi:10.3389/fonc.2018.00008
39. de Lera AR, Ganesan A. Epigenetic polypharmacology: from combination therapy to multitargeted drugs. *Clin epigenetics*. 2016;8(1). doi:10.1186/s13148-016-0271-9
40. Anighoro A, Bajorath J, Rastelli G. Polypharmacology: challenges and opportunities in drug discovery. *J Med Chem*. 2014;57(19):7874–7887. doi:10.1021/jm5006463
41. Zhou Y, Zou Y, Yang M, et al. Highly potent, selective, biostable, and cell-permeable cyclic D-peptide for dual-targeting therapy of lung cancer. *J Am Chem Soc*. 2022;144(16):7117–7128. doi:10.1021/jacs.1c12075
42. Vazquez J, Lopez M, Gibert E, Herrero E, Luque FJ. Merging ligand-based and structure-based methods in drug discovery: an overview of combined virtual screening approaches. *Molecules*. 2020;25:20.
43. Bottegoni G, Veronesi M, Bisignano P, et al. Development and Application of a Virtual Screening Protocol for the Identification of Multitarget Fragments. *Chemmedchem*. 2016;11(12):1259–1263. doi:10.1002/cmdc.201500521
44. Yang D-S, Yang Y-H, Zhou Y, et al. A redox-triggered bispecific supramolecular nanomedicine based on peptide self-assembly for high-efficacy and low-toxic cancer therapy. *Adv. Funct. Mater.* 2020;30(4).
45. Degorce SL, Barlaam B, Cadogan E, et al. Discovery of novel 3-quinoline carboxamides as potent, selective, and orally bioavailable inhibitors of Ataxia Telangiectasia Mutated (ATM) Kinase. *J Med Chem*. 2016;59(13):6281–6292. doi:10.1021/acs.jmedchem.6b00519

46. Li X, Inks ES, Li X, et al. Discovery of the First *N*-hydroxycinnamamide-based histone deacetylase 1/3 dual inhibitors with potent oral antitumor activity. *J Med Chem*. 2014;57(8):3324–3341. doi:10.1021/jm401877m
47. Vickers CJ, Olsen CA, Leman LJ, Ghadiri MR. Discovery of HDAC inhibitors that lack an active site Zn^{2+}-binding functional group. *ACS Med. Chem. Lett*. 2012;3(6):505–508. doi:10.1021/ml300081u
48. Yang YR, Mou Y, Wan LX, et al. Rethinking therapeutic strategies of dual-target drugs: an update on pharmacological small-molecule compounds in cancer. *Med Res Rev*. 2024;44(6):2600–2623. doi:10.1002/med.22057
49. Wang W, Sun Y, Liu XB, et al. Dual-targeted therapy circumvents non-genetic drug resistance to targeted therapy. *Front Oncol*. 2022;12.
50. Tcs H, Chan AHY, Ganesan A. Thirty Years of HDAC Inhibitors: 2020 Insight and Hindsight. *J Med Chem*. 2020;63(21):12460–12484. doi:10.1021/acs.jmedchem.0c00830